Title	Study of Segregation in Alloys Irradiated by Ions and Electrons
Author(s)	Takeyama, Taro; Ohnuki, Soumei; Maruyama, Shigeki
Citation	, 104, 65-76
Issue Date	1981-05-30
Doc URL	http://hdl.handle.net/2115/41679
Type	bulletin (article)
File Information	104_65-76.pdf

Study of Segregation in Alloys Irradiated
by Ions and Electrons

Taro Takeyama,* Soumei Ohnuki*
and Shigeki Maruyama*
(Received December 27, 1980)

Abstract

Radiation induced segregation on binary alloys, 316 stainless steel and ferritic alloys was studied by means of an energy dispersive X-ray microanalyzer attached to a 200 kV STEM. Irradiation was carried out in a 650 kV high voltage electron microscope up to 10 dpa for binary alloys and in 200 kV C^+ ion accelerator up to 57 dpa. The segregation was observed on internal sinks, such as grain boundaries, voids, dislocation loops and precipitates. Radiation induced precipitation was caused by the segregation in unsaturated alloys. The type of segregation or depletion depended primarily on the difference of the size factor. However, unexpected segreration was detected in some alloys irradiated by ions. The segregation and depletion of the solutes could be affected by the nucleation and growth of voids.

1. Introduction

Radiation induced segregation (RIS) near defect sinks causes a compositional change during irradiation and affects void formation and the mechanical properties in alloys. It is considered that RIS is one of the most important points for research in fusion reactor materials. RIS has been considered to be the result of the interaction between point defects and solute atoms, and has been observed in voids [1-2], loops [3] and irradiated surfaces [4]. However, precise studies have not been carried out for internal sinks such as grain boundaries and voids. The aim of this study is to clarify the mode of solute segregation at these sinks irradiated by ions and electrons. The results indicate segregation or depletion at the sinks of binary alloys irradiated by electrons and the information was confirmed in austenitic and ferritic stainless steels irradiated by ions.

2. Experimental Procedure

The alloys and the irradiation conditions are given in Table 1. The binary alloys were irradiated by electrons in high voltage electron microscope (HVEM) at 650 kV. The irradiated area of 10μm in diameter included a vertical grain boundary and one

---

* Metals Research Institute

Table 1 Alloys and irradiation conditions.

Alloys	Dose	Temperature
Electron irradiation		
Cu−2%Fe (at%) Cu−2%Ag Cu−2%Si Cu−2%Ni	∼ 10 dpa	373 ∼ 573 K
Ni−2%Cu (at%) Ni−8%Si Ni−6%Al	∼ 5 dpa	573 ∼ 723 K
Fe−1%Mn (at%) Fe−5%Cr Fe−13%Cr	∼ 3 dpa	573 ∼ 723 K
Ion irradiation		
316 SS	∼ 76 dpa	973 K
Fe−13%Cr (wt%) Fe−13%Cr−1%Si Fe−13%Cr−1%Ti	∼ 57 dpa	798 K

of the grains was either on a {110} or {111} plane. The electron flux was 3×10^{23} e/ m^2s, and the damage rate was $4 \sim 9 \times 10^{-4}$ dpa/s. After irradiation, the irradiated and unirradiated areas in the same grains were analyzed by an energy dispersive X-ray microanalyzer (EDX) attached to a 200 kV STEM. Fig. 1 gives the geometry of the EDX analysis. To determine the concentration profile, we adopted the count ratio method, comparing the result with that of a standard alloy. The ratio was almost proportional to the concentration of the solute. 316 stainless steel, Fe–Cr and Fe–Cr–Si or Ti alloys were irradiated by C^+ in a 200 kV ion accelerator. Irradiation
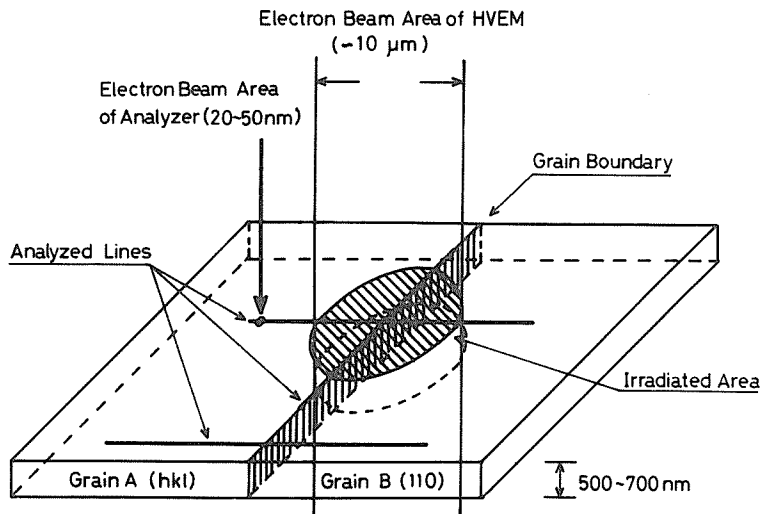
Fig. 1 Schematic illustration showing the geometry of energy dispersive X-ray analysis in electron irradiated and unirradiated areas.

conditions were 76 dpa at 973 K and 57 dpa at 798 K for the austenitic and ferritic alloys, respectively. The damage rate was 6×10^{-3} dpa/s. EDX analyses were carried out for grain boundaries, voids and precipitates.

3. Result and Discussion

3. 1. Electron irradiation

Dislocations, voids and precipitates were produced in copper alloys during electron irradiation at a temperature range from 423 to 573 K. In the irradiation up to 10 dpa at 523 K, which was the peak swelling temperature of pure copper, the void swellings of Cu-Fe and Cu-Ag alloys were 2 and 6 %, and the number densities were 5×10^{19} and 2×10^{20} m^{-3}, respectively. The details of irradiation microstructures will be found elsewhere [5]. As the profile of the radiation induced segregation depends strongly on the temperature, specimens irradiated at higher temperatures were analyzed by EDX. We used the count ratio method of Fe-$K\alpha$/Cu-$K\alpha$ and Ag-$L\alpha$/Cu-$K\alpha$ to determine the concectration profile. Fig. 2 shows the relation between the ratio (Fe/Cu) and the distance from a grain boundary in the irradiated area. The segregation of Fe occurred clearly on the grain boundary. The segregated zone spread to about 300 nm on both sides and a depleted zone of Fe was produced at the outer areas. As the ratio in the unirradiated area was about 3×10^{-2}, the degree of radiation induced segregation on the grain boundary was more than twofold. Sub-peaks were observed
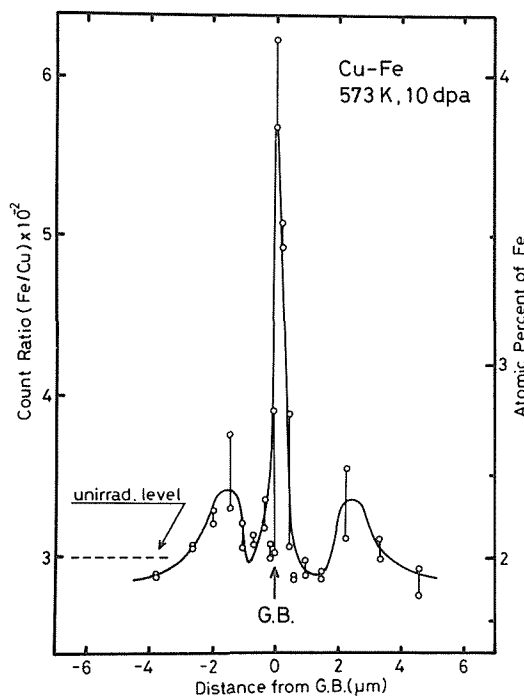

Fig. 2   Relation between count ratio and distance from grain boundary in electron irradiated Cu-Fe alloy. Note the single peak.

at a distance of 2 μm from the grain boundary, which presumably arise from the following reasons. Point defects flow not only to the grain boundary but also to the outer sides in the irradiated area because the defect concentration was higher at the central area than the outer area as a result of the difference of the irradiation electron flux. Moreover, a region with a high dislocation density in the outer area was produced during irradiation by dislocation climb motion, consequently the sub-peaks may be caused by the segregation on dislocations.

Fig. 3 shows the relation between the ratio (Ag/Cu) and the distance from a grain boundary in a typical area irradiated at a dose of 10 dpa at 523 K. A double peak was observed near the grain boundary within a distance of 300 to 500 nm. The difference of the peak heights would be dependent on the damage rate at each grain, because the {110} plane, shown in right hand grain, has a lower threshold energy. At the grain boundary the concentration of Ag was lower than the peak area, therefore, Ag would be depleted at the grain boundary. However, the reason why the concentration at the grain boundary was higher than the unirradiated level would be caused by the lower resolution of the analyzed beam. The depletion of Ag on the outer side of the irradiated area suggests the segregation to the inner side. As the ratio in the unirradiated area was about 3.5×10^{-2}, the degree of radiation induced segregation of Ag was not larger than that of Fe.

The concetration profile of solute atoms near a void was also studied as shown in Fig. 4 and 5. Fe segregated onto a void with a width of 100 nm from the center of the void and then a depleted zone was observed on the outside for about 400 nm. On the other hand, the concentration of Ag decreased near a void and then increased slightly on the outside. The peak of the concentration was at a distance of 120 nm
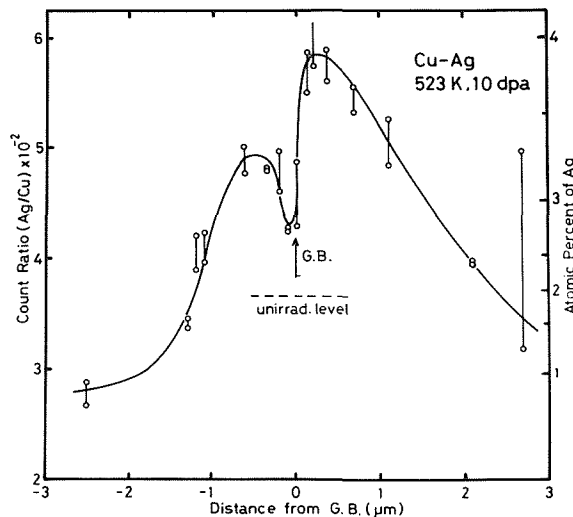

Fig. 3 Relation between count ratio and distance from grain boundary in electron irradiated Cu-Ag alloy. Note the double peak.
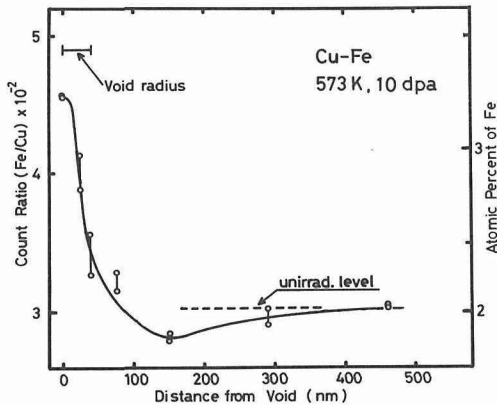
Fig. 4 Segregation profile near void in Cu–Fe alloy. The segregated zone is on the void and the depleted zone is outer area.
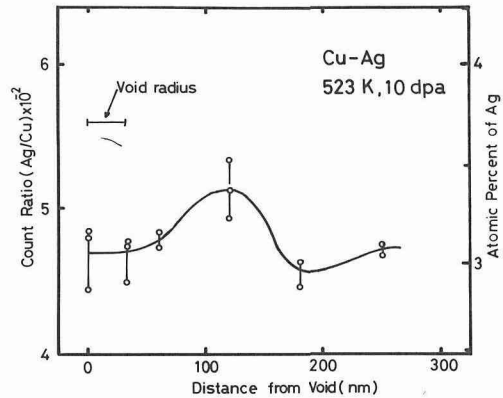

Fig. 5 Segregation profile near void in Cu–Ag alloy. Note the segregated zone is outer area.

from the center of the void. However, the average concentration of an analyzed area was higher than unirradiated level, because the void was formed at the high concentration area shown in Fig. 3. Although the profiles of the segregation near voids were different from each other, it could be concluded that the Fe or Ag enriched shell was produced as a result of the segregation on and near the void, and the extent of the segregation would be larger in the case of the Cu–Fe alloy than Cu–Ag alloy.

In the case of unsaturated Cu–Si alloy [6], fine precipitates were formed in the irradiated area and the depletion of Si was confirmed on a grain boundary. Those precipitates disappeared during annealing after the irradiation on account of radiation induced precipitates as shown in Fig. 6. The migration energy of vacancies in the Cu–Si alloy obtained from the growth speed of loops was larger than that in pure Cu.
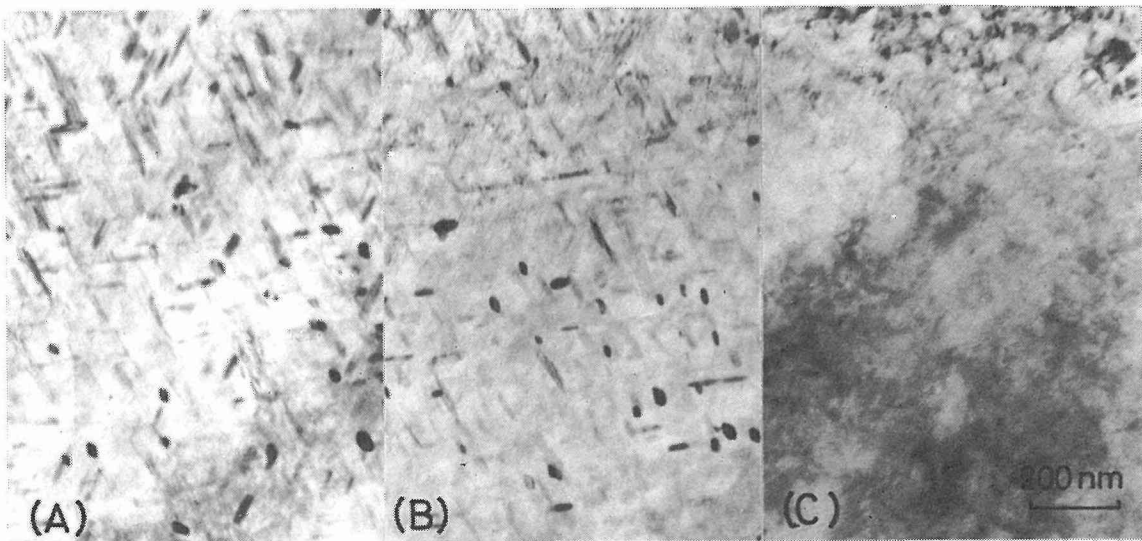

Fig. 6 Thermal stability of radiation–induced precipitates in Cu–Si alloy. (A) as–irradiated condition, 423 K, 10 dpa, (B) annealed at 423 K for 50 min, and (C) annealed at 573 K for 50 min.

The interaction energy between vacancy and Si atom was 0.24 eV. Therefore, RIS of this alloy can be said to be governed by the interaction between vacancies and Si atoms.

In solid solution of Cu and Ni [6], RIS was observed on voids and grain boundaries of both Cu–rich and Ni–rich alloys. In these alloys Ni is an undersized solute and Cu is an oversized one. In the Cu–Ni alloy the " line of no contrast " which is characteristic of a spherical coherent strain was observed around voids, as shown in Fig. 7, but the strain could not observed in the void of Ni–Cu alloy and pure Cu. The concentration profile was also analyzed by EDX. Segregation of Ni on voids was confirmed in Cu–Ni alloy. Therefore, the appearence of the contrast was caused by the strong segregation of Ni atoms on the void. On the contrary, Cu depleted on to voids in Ni–Cu alloy. The RIS on grain boundary was observed as a single peak of Ni and a double peak of Cu.

In the case of the unsaturated Ni–Si and Ni–Al alloys [7], loops were produced at early stages of the irradiation, and then the loops developed into dislocation lines. However, the stability of the loops under the irradiation was different for each alloy. In these alloys Si is an undersized solute and Al is an oversized one. Precipitates of Ni$_3$Si were confirmed on the loops and grain boundaries by the electron diffraction pattern and the dark field image, as shown in Fig. 8, but no precipitate was observed in the Ni–Al alloy. EDX results showed that Si segregated and Al depleted on grain boundaries in these alloys. Therefore, it is suggested that the RIS contronls the growth of the loops due to the segregation of solute, and consequently the development
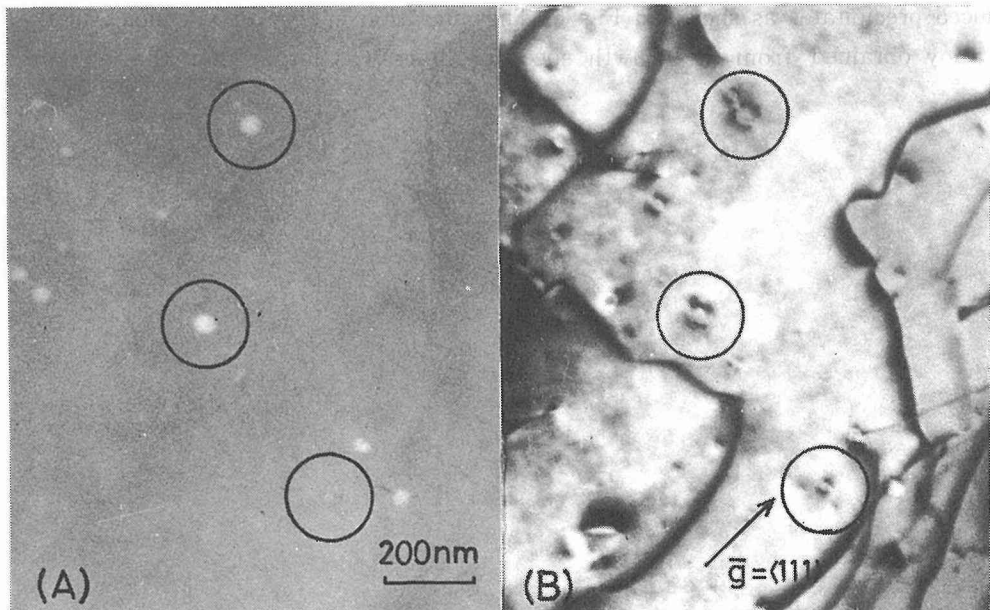
Fig. 7 Void contrast in Cu–Ni alloy irradiated to 7 dpa at 573 K. (A) absorbed condition, and (B) diffracted condition. Note the coherent strain field around void.
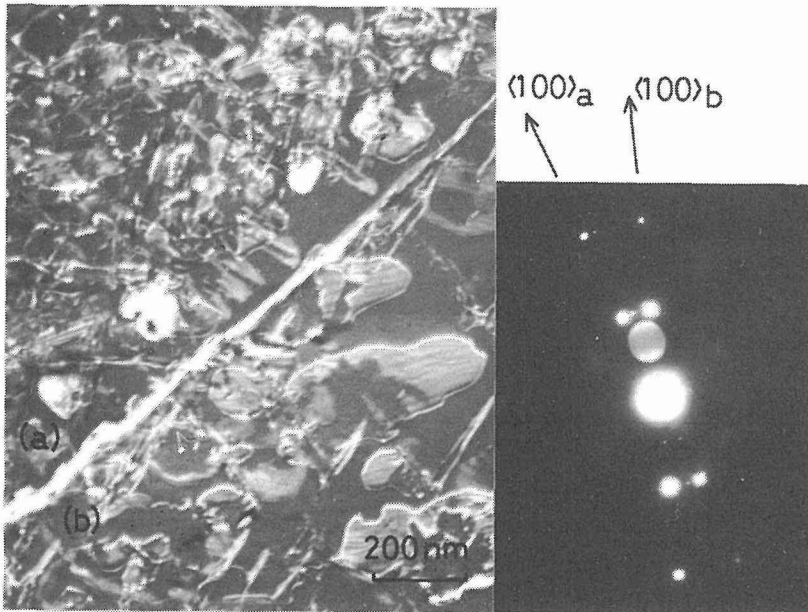
Fig. 8　Dark field image of Ni$_3$Si in Ni–Si alloy irradiated to 3.3 dpa at 723 K.

of the loops in Ni–Si alloy could be delayed.

In the case of Fe–Mn alloy [8], undetermined phases were observed on grain boundaries during irradiation and Mn was depleted at the grain boundaries. From the results on the loop growth, the interaction energy between a vacancy and a Mn atom was estimated to be 0.15 eV. Therefore, it can be said that the RIS is controlled by vacancy migration. In the case of Fe–5%Cr and Fe–13%Cr alloys, Cr was also depleted on grain boundaries and in this case the extent of the depletion increased with the increase of Cr concentration, as shown in Fig. 9. The results of RIS in electron irradiated alloys are summarized in Table 2.
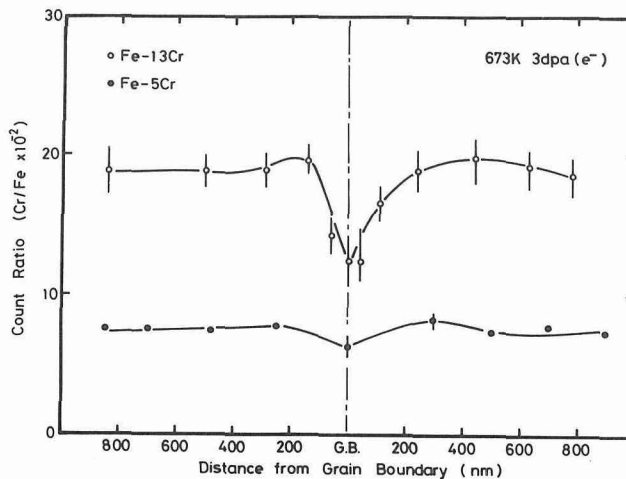
Fig. 9　Segregation profile near grain boundary in Fe–5%Cr and Fe–13%Cr alloys electron irradiated to 3 dpa at 673 K.

'Table 2   RIS and microstructures of binery alloys irradiated by electrons.

Alloy	Segregation or Depletion	Sinks	Microstructures
Cu−Fe	S	G and V	P and V
Cu−Ag	D	G and V	P and V
Cu−Si	D	G	P and V
Cu−Ni	S	G and V	V
Ni−Cu	D	G and V	V
Ni−Si	S	G and L	P
Ni−Al	D	G	
Fe−Mn	D	G	
Fe−Cr	D	G	

S: segregation   D: depletion   G: grain boundary   V: void   L: loop   P: precipitate

The RIS of substitutional solutes can be qualitatively explained by the size factor [4, 9, 10]. The first mechanism assumes a mixed dumbbell migration of an underiszed solute with a self–interstitial atom, which causes a solute segregation in the same direction as the self–interstitial flow. The second mechanism is a result of an exchange of an oversized solute atom with a vacancy, which leads to a preferential flow of the solute in the opposite direction of the vacancy flow and this causes depletion in sinks. Fig. 10 illustrates RIS mechanism from the point of view of the defect–solute interaction. As mentioned above, RIS occurring at defect sinks in electron irradiated fcc and bcc alloys can be classified into segregation and depletion types depending primarily on the difference of the size factors.

Fig. 11 gives a schematic illustration of the solute concentration profile near voids. In these experiments, the voids have a shell of higher solute segregation in undersized alloys than the observed ones. The nulceation and growth of voids would be strongly
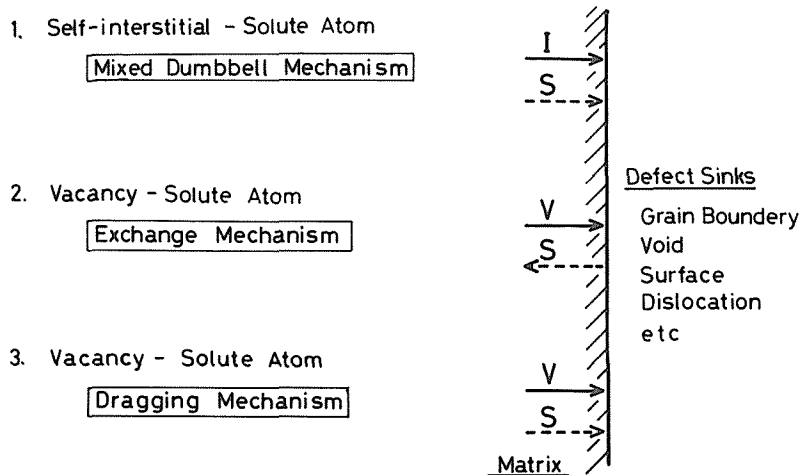
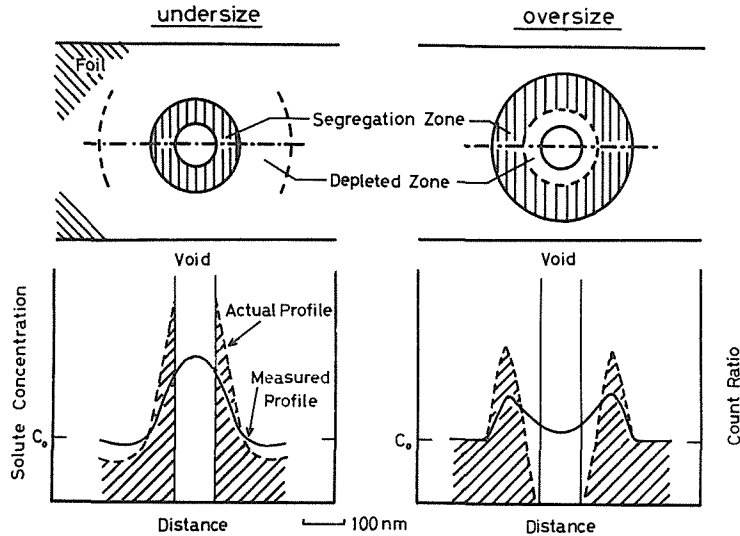Fig. 10   Interaction between irradiation defects and solute atoms.

Fig. 11 Segregation profiles near voids in under and oversized alloys. Solid curves indicate the measured profiles and dotted curves show actual ones.

affected by the segregation [5]. Wolfer [8] suggested that segregation changes the image interaction between point defects and voids, in addition to having the effect of reducing the surface energy.

Our results show that void swelling and void number density depend on the behavior of RIS, because of a tendency in which void swellings of undersized alloys are smaller than for others. When RIS occurred near voids, the flow of defects to them would be disturbed by the shell of segregation, and consequently the growth of voids could be suppressed.

3. 2. Ion irradiation

316 stainless steel is a commercial alloy used in a fast breeder reactor. In this alloy the RIS of elements at external surfaces and other defect sinks has become a commonly observed effect, however, the effect of the RIS on the void formation is not clear. For 316 stainless steel irradiated by C^+ ions [12], dislocations and two types of void were observed. It is deduced that the large voids were formed at the initial stage of the irradiation and the small ones with high number density associated with dislocations. The large voids have a void free zone of 70 nm width. Solute segregation profile was determined around the large voids, as shown in Fig. 12. Cr depleted strongly, but Ni, Si, Mo and Ti segregated to void surfaces. The width of the segregation or depletion zone was about 100 nm and was also the same width as the void free zone. This fact suggests that the segregation and depletion of solutes could affect the formation of small voids.

Ferritic alloys are candidate materials for a fusion reactor, but are sensitive to the alloying element with regard to mechanical properties and the behavior of irradiation-induced defects. The ferritic alloys irradiated by C^+ ions [13] had no voids, and

precipitates were formed during irradiation as shown in Fig. 13. For Fe–Cr alloy, Cr-rich precipitates were observed in the matrix and on grain boundaries. The micro-structures of Fe–Cr–Si alloy consisted of two types of precipitate at 30 dpa, the large
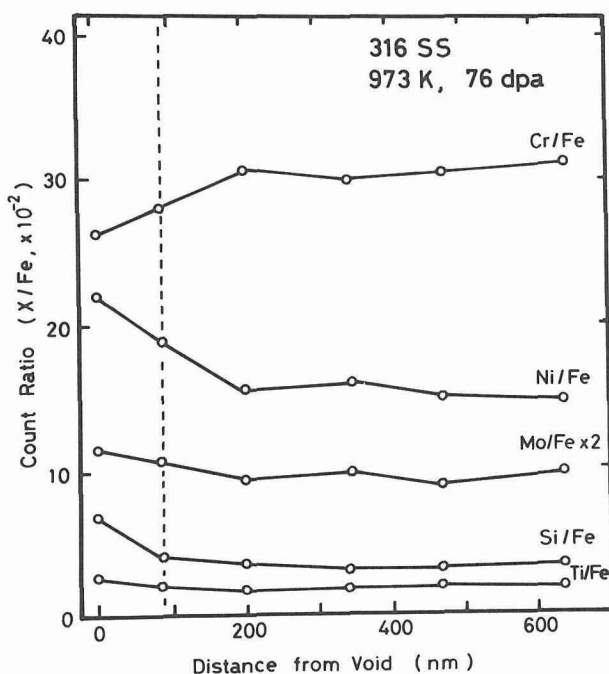

Fig. 12 Segregation profile of solutes around void in ion irradiated 316 stainless steel.
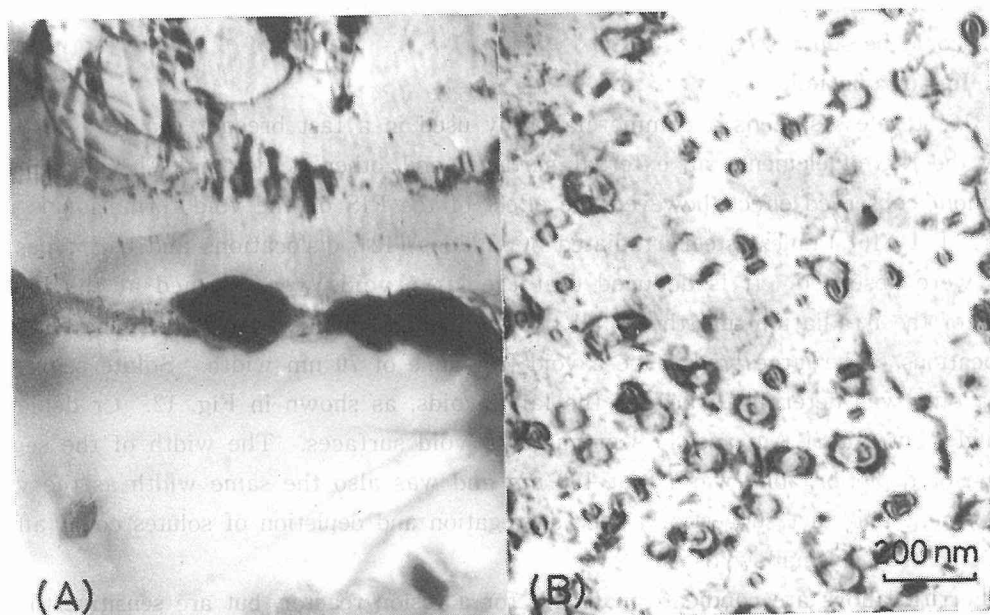

Fig. 13 Microstructures of ferritic alloys irradiated by ions at 798 K. (A) Fe –13%Cr, 57 dpa, and (B) Fe–13%Cr–1%Ti, 57 dpa.

ones were enriched in Cr and Si, and the small ones were enriched only in Cr. The larger ones had a precipitation free zone, and after 57 dpa only large precipitates were observed. For a Fe–Cr–Ti alloy, only small Ti–rich precipitates were observed with a high number density.

At the grain boundaries the RIS behavior changed with the ion irradiation as shown in Fig. 14~15. For Fe–Cr and Fe–Cr–Si alloys, Cr and Si were enriched on the grain boundaries, but the concentration of Cr was lower in Fe–Cr–Si alloy than Fe–Cr alloy as a result of Si segregation. However, for Fe–Cr–Ti alloy, the depletion of Cr and enrichment of Ti were observed on the grain boundaries. The results of the ion irradiation are summarized in Table 3. From the size factor, it is expected that the depletion of Cr and the segregation of Si and Ti would occur at defect sinks in these binary ferritic alloys. However, the RIS behavior of the alloys irradiated by ions does
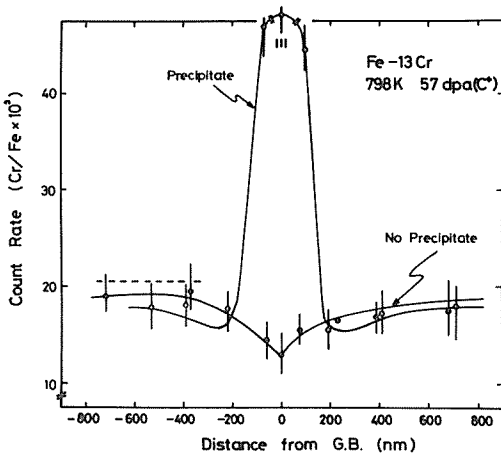

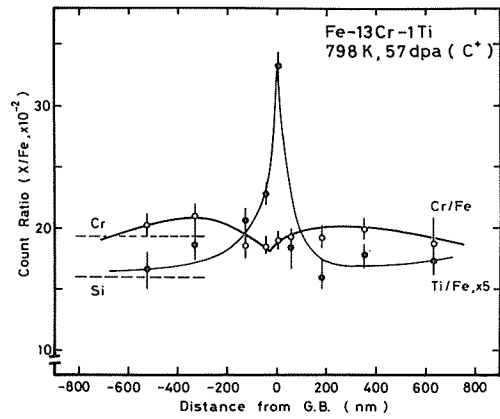**Fig. 14** Segregation profile in ion irradiated Fe–13%Cr alloy.

Fig. 15 Segregation profile in ion irradiated Fe–13%Cr–1%Ti alloy.

Table 3 RIS and microstructures of austicnitie and ferritic alloys irradiated by C^+ ions.

Alloy	Alloying Element	Segregation or Depletion	Sinks	Microstructures
316 SS	Cr	D	V	
	Ni	S	V	
	Mo	S*	V	
	Si	S	V	
	Ti	S	V	
Fe–13%Cr	Cr	S*	G	P (Cr–rich, M and G)
Fe–13% Cr–1% Si	Cr	S*	G	Small P (Cr–rich, M)
	Si	S	G	Large P (Cr and Si–rich, M and G)
Fe–13% Cr–1% Ti	Cr	D	G	Small P (Ti–rich, M and G)
	Ti	S	G	

S: segregation   D: depletion   G: grain boundary   V: void   M: matrix   P: precipitate
*unexpected segregation

not follow the simple model. To solve the problem of this unexpected RIS, the interactions among defects, major and minor solute atoms must be clarified. Moreover, the effects of irradiation conditions, such as damage rate, dose and temperature, must be considered.

4. Conclusions

Radiation induced segregation was studied by means of EDX on alloys irradiated by C^+ ions and electrons.

1) RIS was observed on internal sinks, such as grain boundaries, voids, dislocation loops and precipitates.

2) Segregation and depletion types depended primarily on the difference of the size factor.

3) Precipitation was caused by RIS in unsaturated alloys.

4) Unexpected segregation was detected in some alloys irradiated by ions.

5) The segregation and depletion of solutes could affect the nucleation and growth of voids.

Acknowledgement

References

[1] T. Takeyama, S. Ohnuki and H. Takahashi, Scripta Met., 14 (1980) 1105.

[2] H. Takahashi, S. Ohnuki and T. Takeyama, J. Nucl. Mater., 96 (1981) 233.

[3] A. Barbu and G. Martin, Scripta Met., 11 (1977) 771.

[4] P. R. Okamoto and H. Wiedersich, J. Nucl. Mater., 53 (1974) 336.

[5] T. Takeyama, S. Ohnuki and H. Takahashi, ibid., 89 (1980) 253.

[6] T. Takeyama, S. Ohnuki and H. Takahashi, to be published.

[7] T. Takeyama, S. Ohnuki and T. Ebe, to be published.

[8] T. Takeyama, S. Maruyama, S. Ohnuki and H. Takahashi, to be published.

[9] H. W. King, J. Mater. Sci., 1 (1966) 79.

[10] R. A. Johnson and N. Q. Lam, Phys. Rev., B15 (1977) 1794.

[11] W. G. Wolfer, in : Proc. Intern. Conf. on Fundamental Aspects of Radiation Damage in Metals, Gatlinburg, TN, 1975, Conf–751006–P2, p. 812.

[12] M. Terasawa, S. Nakahigashi, T. Takeyama, S. Ohnuki and H. Takahashi, to be published.

[13] S. Ohnuki, H. Takahashi and T. Takeyama, to be published.